COMPLEX TERRAIN MODULE

CERC

In this document 'ADMS' refers to ADMS 6.0. Where information refers to other models, the model name is given in full.

CONTENTS

1.   Introduction

2.   FLOWSTAR

3.   Flow around hills in Stable Conditions

4.   Regions of Reverse Flow

5.   Concentration Calculations

6.   Example Model Output

7.   References

1.   Introduction

The ADMS complex terrain module models dispersion over hills and regions with varying surface roughness. The flow and turbulence fields over the complex terrain are calculated, and used to adjust the plume height and plume spread parameters calculated by the flat terrain model. The model takes account of all common cases where the 'mean' wind dominates the flow. It does not take account of thermal winds.

 In most situations the flow and turbulence fields are calculated using the FLOWSTAR model, which is described in Section 2. In very stable conditions, the flow field may divide, with air at low levels flowing around rather than over the hills. The treatment of these conditions in ADMS is described in Section 3. Section 4 outlines the treatment of plumes emitted into regions of reverse flow. Section 5 describes the adjustment of the plume parameters, once the flow field has been calculated.

2.   FLOWSTAR

2.1   Introduction
FLOWSTAR calculates the flow field and turbulence parameters over complex terrain using linearised analytical solutions of the momentum and continuity equations. An overview of the calculation procedure is given below. A full description of the underlying theory is given in Appendix A.

2.2   Input data
As input, FLOWSTAR requires data on the terrain height and surface roughness. FLOWSTAR uses the same meteorological data as the main ADMS model. Boundary layer parameters are calculated using the ADMS boundary layer structure module.

In line with the assumptions on which the model is based, the model can typically be used for gradients up to about 1:2, but may not be reliable close to isolated slopes or escarpments with higher gradients or more generally if large parts of the modelling domain have gradients greater than 1:2. Usually it is advisable to include terrain height effects if the gradients exceed 1:10 in the model domain.

The data input by the user in the terrain file can be at any grid size, and the grid does not have to be regular. However, the maximum number of data points in the terrain file is 770,000.

The input terrain data file takes the following form:

$$
\begin{array}{llll}
1, & x_1, & y_1, & z_1 \\
2, & x_2, & y_2, & z_2 \\
\cdot & \cdot & \cdot & \cdot \\
\cdot & \cdot & \cdot & \cdot \\
i, & x_i, & y_i, & z_i \\
\cdot & \cdot & \cdot & \cdot \\
\cdot & \cdot & \cdot & \cdot \\
n, & x_n, & y_n, & z_n
\end{array}
$$

where i is the index (number) of the point with position (x_i, y_i) and z_i is its elevation. For example, in a domain 20km x 20km with 4096 regularly spaced points of data the terrain would be specified at points approximately 320m apart.

If the surface roughness varies across the domain, surface roughness data may be entered in the same way. If the roughness is assumed constant across the domain, one value is supplied to the model, rather than gridded data.

2.3   Calculation methodology

For each wind direction a wind-aligned rectangle is described around the terrain points. Points in the corners of the wind-aligned rectangle are assigned the mean terrain height over the boundary of the user input domain. An internal calculation grid is set up over the rectangle. This grid is regularly spaced and may have up to 512x512 points in the horizontal, the resolution being selected by the user in the model interface. The number of points on the calculation grid affects the model speed, memory requirement and model solution. A 64x64 grid is recommended for most practical applications with slopes up to 1:3 if the domain is not large (not more than 10 km x 10 km). The grid has 17 vertical levels ranging from 1.3 times the minimum surface roughness to 5 km.

Fourier transforms of the terrain and roughness data are calculated and the flow solution is calculated by inverting the Fourier transformed solution. In these calculations, the atmosphere is split into three layers:
i)   the *inner layer*, close to the ground, where shear stress perturbations must be taken into account but stratification is unimportant
ii)   the *middle layer*, far enough from the ground that shear stresses are not important but the effects of stress are; again stratification is unimportant
iii)   the *outer layer*, where shear is unimportant, but stratification must be taken into account.
Two stratification cases are considered in ADMS, corresponding to stable conditions with a uniform density gradient and neutral or unstable conditions where there is an inversion and discontinuity in density at a certain height h, constant density below h and a uniform density gradient above h.

2.4   Output
The outputs of the model are:

(i)   local mean wind velocity components $(U + u, v, w)$

(ii)   local root mean square velocity scales $\sigma_u, \sigma_v, \sigma_w$

(iii)   vertical and transverse length scales L_W and L_v

(iv)   Lagrangian time scale T_L

(v)   energy dissipation rate ε

These variables are used to adjust the plume parameters calculated by the flat terrain model (see Section 5).

3.   Flow around hills in Stable Conditions

3.1   Introduction

It is well established [14] that when stable flows approach an isolated hill the flow may divide, with the air above a certain height h_c (the 'dividing surface') flowing over the hill and air below h_c flowing around the hill, see Figure 3.1.
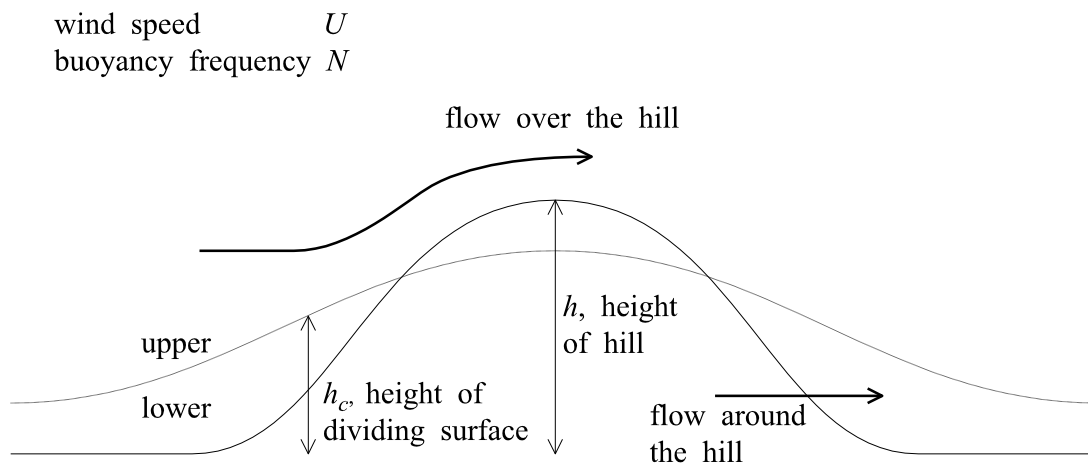

Figure 3.1   Different flow regimes above and below the dividing streamline. H_c is the maximum height of the dividing surface.

If the maximum height of the dividing surface, H_c is greater than 20 m then there is assumed to be flow around the hill, calculated as described in section B2. This stable flow field is then used in the plume dispersion calculations, with corrections very close to the ground. If $H_c < 20$m then the usual FLOWSTAR flow field is used.

When considering real terrain data including multiple hills, there are difficulties in defining a dividing surface and combining flow solutions for each hill. In ADMS, a simplified method is adopted: in stable conditions a dividing surface is defined based on the highest hill, and if H_c is greater than 20 m an alternative flow field is calculated using the method outlined in Section 3.2. Further details can be found in section B2.

3.2   Calculation methodology

To calculate the flow field, the terrain data is simplified to a single Gaussian shaped hill of circular cross section. Its height is taken to be the height of the highest hill, and the horizontal length scale is the characteristic length scale of the terrain as calculated by FLOWSTAR. Then a dividing surface is defined, also Gaussian in shape and based on the single idealised hill. Below the dividing surface, the flow is approximated by assuming horizontal potential flow around a cone of radius $r(z)$, the radius of the hill at height z, apart from upstream flow in a thin layer close to the terrain where a 'parallel flow' solution is used. Above the dividing surface, the flow field is taken from the FLOWSTAR solution, with a correction for flow near the ground.

4. Regions of Reverse Flow

4.1 Introduction

A source located within a region of reverse flow (i.e. a region where the wind velocity component in the free stream wind direction is negative) may lead to high concentrations upstream of the source.

In ADMS it is assumed that a plume released into a reverse flow region is well-mixed within that region. The release is represented downwind of that region by dispersion from a virtual source. This is closely analogous to the treatment of plumes entrained into the near wake ('recirculating region') of a building in the ADMS buildings module. However, unlike the buildings module, the case of a plume being partially entrained into the near wake is not treated. Currently only plumes released into a reverse flow region are treated – the plume is not permitted to enter a reverse flow region after release.

4.2 Calculation methodology

An 'effective source height' is defined, which includes the initial effects of buoyancy and momentum of the release. If the downwind velocity component at the effective source is negative (i.e. the effective source is in a reverse flow region), then the full extent of the reverse flow region is found. An 'effective recirculation zone' is then defined (Figure 4.1), throughout which the contaminant is assumed to be well-mixed. The concentration is assumed to be uniform within this 'effective recirculation zone'. The effective recirculation zone may be the same as the recirculation zone or may be contained within it, for instance if the zone is very wide.

At the downstream edge of this zone, the plume dispersion parameters (σ_y and σ_z are estimated based on the cross-stream dimensions of the effective recirculation zone. These parameters are used in the subsequent calculations of plume concentration to represent dispersion from a 'virtual source', or a number of 'virtual sources' if the original source has a large crosswind extent. The plume from each virtual source is assumed to be passive.

For an effective source outside the reverse flow region the plume dispersion calculations are influenced by a reverse flow region only if the plume centre line enters the region. No partial entrainment of the plume is assumed. If reverse flow is encountered by the plume centreline, then the plume height is increased until it is within a region of forward flow.

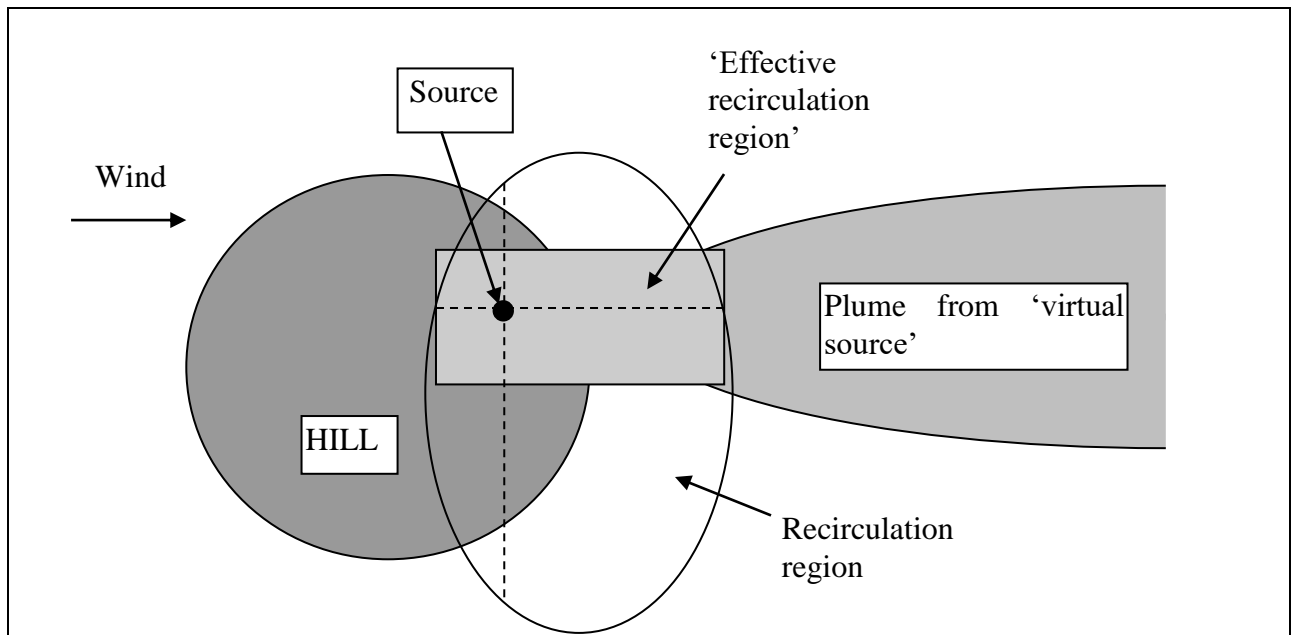Full details of the calculation procedure are given in Appendix C.

Figure 4.1 The recirculating region and effective recirculating region

5.   Concentration calculations

5.1   Introduction
To calculate concentrations over complex terrain, the calculated flow and turbulence fields are used to make adjustments to the plume height and plume spread parameters. Concentration calculations then proceed using the same methods as the flat terrain module.

5.2   Plume centreline height
In the ADMS flat terrain module, the change in plume height between downstream calculation points x_1 and x_2, say, includes contributions from plume rise and gravitational settling. In the complex terrain module, an extra contribution from the terrain effects is included. This is calculated by following a streamline downwind from the initial plume position. The wind velocity field at the initial plume centreline position $(x_1,\ y_1,\ z_1)$ is calculated by linear interpolation between points on the FLOWSTAR calculation grid.   The model then steps downstream along the streamline to x_2 to calculate the adjusted crosswind plume position y_2 and plume centreline height z_2.   With variable roughness, the velocity profile near the ground is adjusted to be zero at the local roughness height.

5.3   Plume spread parameters
The technique used here is similar to that used in the ADMS Buildings module. Firstly the plume spread parameters over flat terrain are calculated. The plume spread parameters over complex terrain are then calculated from the flat terrain values using differential equations taking account of changes in mean wind speed and turbulence due to the terrain:

$$\frac{d}{dx}(\sigma_{yh}) = \frac{\left\{1 + \frac{\Delta\sigma_v{}^2}{\sigma_{v0}{}^2}\right\}^{1/2}}{\left\{1 + \frac{\Delta u}{U_0}\right\}} \frac{d}{dx}(\sigma_{yf}) \tag{5.1}$$

$$\frac{d}{dx}(\sigma_{zh}) = \frac{\left\{1 + \frac{\Delta\sigma_w{}^2}{\sigma_{w0}{}^2}\right\}^{1/2}}{\left\{1 + \frac{\Delta u}{U_0}\right\}} \frac{d}{dx}(\sigma_{zf}) \tag{5.2}$$

where

$$\Delta u = U - U_0 \tag{5.3}$$

$$\Delta\sigma_v{}^2 = \sigma_{vh}{}^2 - \sigma_{v0}{}^2 \tag{5.4}$$

$$\Delta\sigma_w{}^2 = \sigma_{wh}{}^2 - \sigma_{w0}{}^2 \tag{5.5}$$

U_0 is the unperturbed wind speed, U is the terrain influenced wind component in the free stream direction, σ_{v0} and σ_{w0} are the unperturbed turbulence parameters, and suffices f and h refer to flat and complex terrain.

6.   Example Model Output

Example flow and concentration fields for a simple Gaussian hill are shown below. The input terrain is illustrated in Figure 6.1. The terrain has been modelled under neutral meteorological conditions, with a westerly wind of speed 5 m/s. The resulting flow field at 10 m above the terrain is illustrated in Figure 6.2.

A source of height 50 m with a passive release of 1 g/s was included at (-1000, 500). Figure 6.3 shows the resulting ground level concentrations.
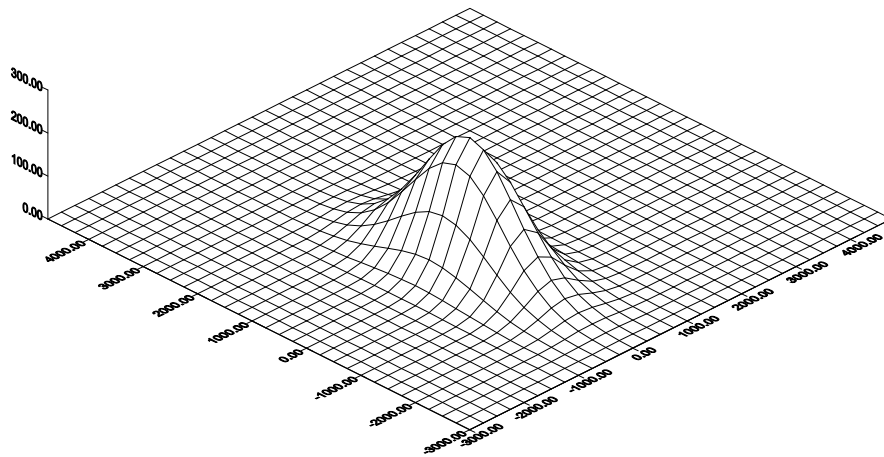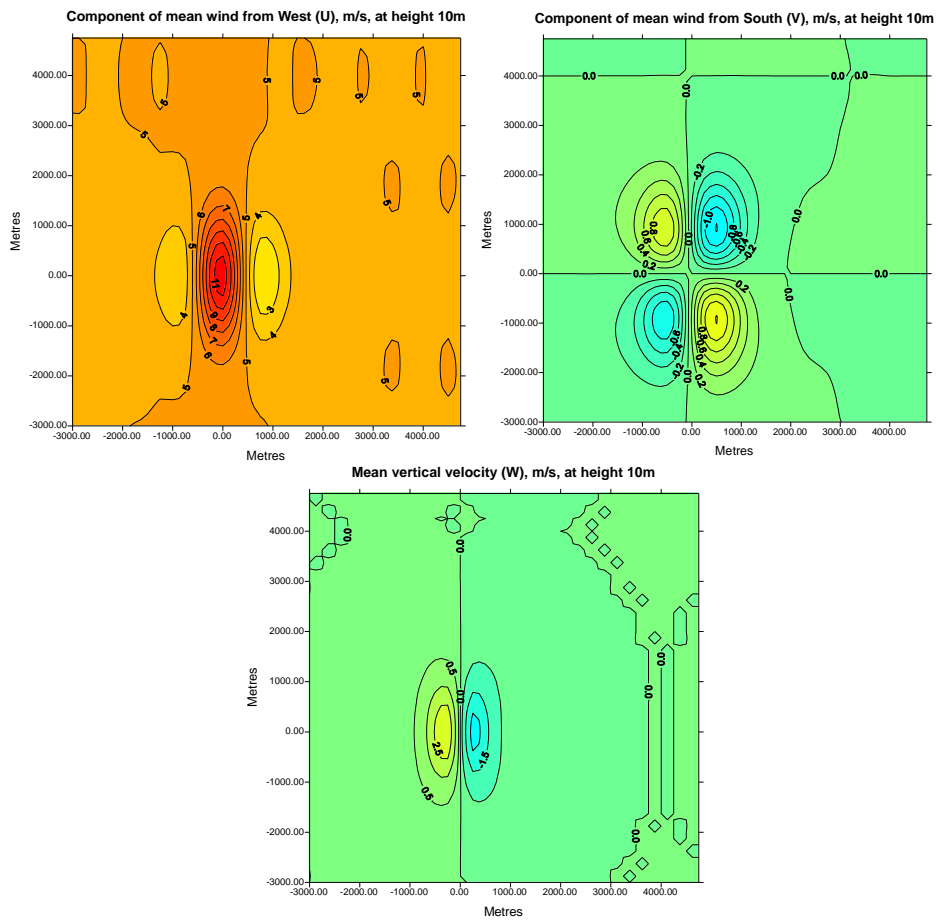
Figure 6.1 Input terrain data

Component of mean wind from West (U), m/s, at height 10m

Component of mean wind from South (V), m/s, at height 10m

Mean vertical velocity (W), m/s, at height 10m

Figure 6.2 Wind field at 10 m above terrain, neutral conditions
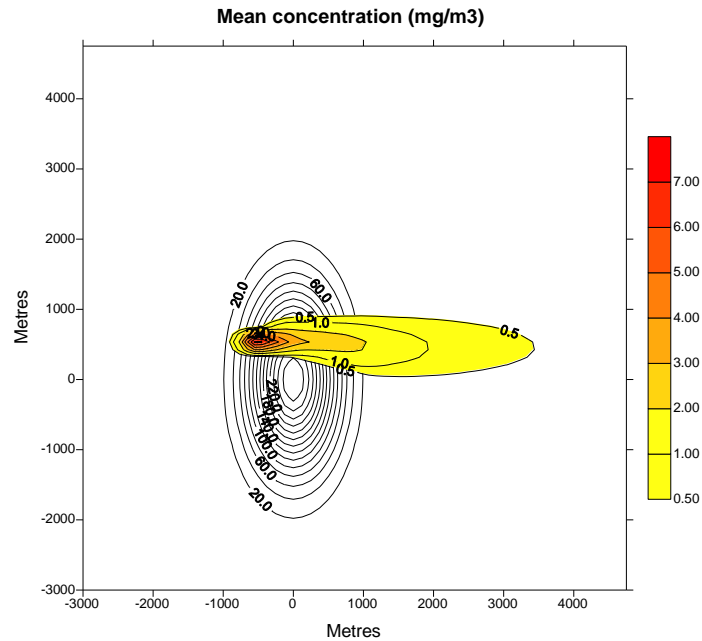
Mean concentration (mg/m3)

Figure 6.3 Ground level concentrations from a 50m release at (-1000, 500), overlaid on terrain data

6.   References

[1]   Hunt, J.C.R., Richards, K.J. & Brighton, P.W.M. **1988a**. Stably stratified shear flow over low hills. *Q.J.R. Meteorol. Soc.* **114**, 859-886.

[2]   Hunt, J.C.R., Leibovich, S. & Richards, K.J. **1988b**. Turbulent shear flow over hills. *Q.J.R. Meteorol. Soc.* **114**, 1435-1470.

[3]   Belcher, S.E., Xu, D.P. & Hunt, J.C.R. **1990** The response of the turbulent boundary layer to arbitrarily distributed surface roughness changes. *Q.J.R. Meteorol. Soc.* **116**, 611-635.

[4]   Jackson, P.S. & Hunt, J.C.R. **1975**. Turbulent wind flow over a low hill. *Q.J.R. Meteorol. Soc.* **101**, 929-955.

[5]   Walmsley, J.L., Taylor, P.A. & Keith, T. **1986** A simple model of neutrally stratified boundary layer flow over complex terrain with surface roughness modulations. *B.L. Met.* **36**, 157-186.

[6]   Smith, R.B. **1980**. Linear theory of stratified hydrostatic flow past an isolated mountain. *Tellus* **32**, 348-364.

[7]   Carruthers, D.J. & Choularton, T.W. **1982** Airflow over hills of moderate slope. *Q.J.R. Meteorol. Soc.* **108**, 603-624.

[8]   Hunt, J.C.R. & Richards, K.J. **1984**. Stratified airflow over one or two hills. *B.L. Met.* **30**, 223-259.

[9]   Wieringa, J. **1976** An objective exposure correction method for average wind speeds measured at a sheltered location. *Q.J.R. Meteorol. Soc.* **10**, 241-253.

[10]   Abramowitz, M. & Stegun, I.A. **1972** Handbook of Mathematical Functions. Dover Publications Inc., New York.

[11]   Finnigan, J.J. **1988** Airflow over complex terrain. In **Flow and Transport in the Neutral Environment**: Advances and Applications (eds. W.K. Steffen and O.T. Denmead). Springer-Verlag, Heidelberg.

[12]   Carruthers, D.J. & Hunt, J.C.R. **1990** Fluid mechanics of airflow over hills: Turbulence, fluxes and waves in the boundary layer. AMS Monograph.

[13]   Hunt, J.C.C., Holroyd, R.J. & Carruthers D.J. **1988** Preparatory studies for a complex dispersion model. Report to NRPB, AWE, HMIP, HSE. CERC Ltd.

[14]   Weng, W.S., Richards, K.J. & Carruthers, D.J. **1988** Some numerical studies of turbulent airflow over hills. Proc. 2nd European Turbulence Conf. Aug. 1988 (eds. Fernholz & Fiedler).

[15]   Hunt, J.C.R. **1985** Turbulent diffusion from sources in complex flows. *Ann. Rev. Fluid Mech.* **17**, 447-485

[16]   Lavery, T.F., Bass, A., Strimaitism, D.G., Venkatram, A., Green, B.R., Drivas, P.J., & Egan, B.A. **1981** EPA complex model development. 1st Milestone Report.

[17]   Newley, T.J. **1986** Turbulent airflow over hills. Ph.D thesis, Cambridge University.

APPENDIX A: Description of FLOWSTAR algorithms

Contents

A1. Summary

This note describes the algorithms for the computer model FLOWSTAR which has been developed for predicting the mean flow and mean streamlines in turbulent, stratified flow over hills and roughness changes. The airflow model uses linearised analytical solutions of the momentum and continuity equations, and includes the effects of stratification on the flow. The model is most accurate for hills of moderate slope and can typically be used for gradients up to about 1:2, but may not be reliable close to isolated slopes or escarpments with higher gradients or more generally if large parts of the modelling domain have gradients greater than 1:2. The model can be used for all typical changes in surface roughness, but note that the model does not allow for canopy flows which means that the flow near the ground may not be well represented for the highest roughnesses (e.g. Z_0 > 1.0m). The influence of the terrain and surface roughness changes will vary with the source height and position and the local meteorology.

A2. Overview of the Model and the Computational Procedure

A2.1 Background and previous work

Recently research has shown that analytical solutions can be derived to the governing equations for the mean atmospheric flow over hills and roughness changes given certain assumptions:

(i)   the slopes of the hills are small,

(ii)   the profile of potential temperature $\theta(z)$ in the atmosphere can be approximated to one of five basic forms (defined in §A3.3.2) although only two are used in ADMS,

(iii) the upwind velocity profile increases from the ground upwards and does not have a strong elevated shear layer,

(iv)   the upwind conditions vary slowly on a time scale comparable with that taken by a fluid particle to cross the flow region under consideration. (For a 20 km long region and a wind of 10 m/s, this means slow changes over half an hour.)

(v)   rapid cooling or heating of the surface of the hillside is absent; this can induce significant motions which are not considered here,

(vi)   the turbulent shear stress near the surface can be approximated by the *mixing length* relations between shear stress and velocity gradient.

Using these assumptions, [1]-[3] Hunt et al and Belcher et al have derived formulae for the Fourier transforms of the perturbation (or changes) in the velocity distribution over the terrain. To evaluate the actual flow, the Fourier transforms have to be inverted, usually numerically. These papers are based on earlier studies for neutral flow over hills [4]-[5], for roughness changes [5], and for stratified flows over hills of low slope [6]-[8]. The use of the Fourier transform technique to calculate flows over arbitrary terrain was pioneered by Walmsley et al [5], but it was restricted to *neutral* flow and was based on the earlier and less accurate model of Jackson & Hunt [4].

To understand the aim of the model, it is helpful to explain why it is different to models based on computing the full equations of motion (e.g. PHOENICS, FLUENT, etc). In the full computations, it is necessary to solve seven differential equations for seven variables at each point in the flow domain. So the minimum storage for a 64^3 grid is 7×64^3. By contrast, the computer storage required for the Fourier transform of the terrain is 64×64. The computer time required by the model is therefore also greatly reduced. Then the Fourier transform is inverted to calculate the actual flow variables at any point in the calculation domain, without the need for iteration and there is no doubt about the convergence of the solution once the algorithm and its assumptions have been agreed. This is why the Fourier transform method is quite appropriate for use on desktop computers.

We now introduce the physical ideas behind the three-layer model for the flow.

A2.2 Description of the analytical model and its physical implications

In the solution for the airflow over hills used to produce the algorithms, the lower atmosphere is divided into three layers: the **inner layer**, the **middle layer** and the **outer layer**.

The **inner layer** contains the layer near the ground in which the perturbation shear stresses are important. Using a closure based on local equilibrium of turbulence for the shear stress, Bessel equations are obtained for the perturbation velocities.

The **middle layer** is sufficiently far above the ground that shear stresses are unimportant. However, the effects of shear are important. In both the inner layer and the middle layer the effect of local stratification is not significant, as air flows over the hill, although stratification may affect the upwind profile.

The **outer layer** contains the outer part of the turbulent boundary layer and may also include part of the free, non-turbulent atmosphere (e.g. in case S_2, defined in §A3.3.2, the air above the inversion is generally non-turbulent and does not form part of the boundary layer). In the **outer layer** stratification now has an important effect but the shear and perturbation stress are unimportant. In this layer we solve the equations for **inviscid** stratified flow. For example, the equation for w, in 3-D, is

$$\left\{ \frac{\partial^2}{\partial x^2} \nabla^2 + \frac{N^2}{U_0^2} \nabla_H^2 \right\} w = 0$$

where

$$\nabla^2 = \frac{\partial^2}{\partial x^2} + \frac{\partial^2}{\partial y^2} + \frac{\partial^2}{\partial z^2} \; and \; \nabla_H^2 = \frac{\partial^2}{\partial x^2} + \frac{\partial^2}{\partial y^2}$$

Note that to a first order approximation it is the pressure field developed in the **outer layer** at the boundary with the middle layer which drives the flow in the two lower layers. This pressure field is strongly affected by stratification and so by this means flow in the lower layer is affected by stratification in the **outer layer**.

In the neutral case, there is no stratification and the solution in the *outer layer* is potential flow; the difference is confined close to the hill surface. Before describing the effects of discontinuities in stratification we consider the stable case where there is uniform stratification (i.e. the buoyancy

frequency N is constant with height). The equation shows that waves with frequency $\omega(= U_0 k) < N$ can propagate whilst waves with frequency $\omega > N$ are evanescent and thus decay away from the surface. An upper boundary conditions has to be used for low frequency waves $(\omega < N)$, so that energy propagates upwards. This gives a downward phase velocity and the familiar asymmetrical flow pattern with the strongest velocities downwind of the summit of the hill. The amount of flow moving in horizontal planes around the hill increases with stratification.

In the second kind of stratification considered here, suitable for unstable conditions, there is an inversion at height z_i. Above z_i the air is still stably stratified. Then waves with frequency $\omega > N$ can propagate *within* and along the inversion layer but not in the upper layer above z_i or the middle layer below z_i. It is found that energy may be trapped giving large-amplitude perturbations which, in the atmosphere, appear downwind of the hill. In the linearised mode we have to make an assumption about the amplitude of these resonant waves. We take a plausible value, but recognise that this question has not been properly considered so far.

A2.3 Main elements in the computational model, software and user procedures

There are three main elements in the program and software to implement the model.

(i)   **Input**
        Receiving and storing the data about the terrain, roughness and meteorology (or upwind flow). The data must be specified within a rectangular grid, but can be specified on grid lines with irregular spacing.

(ii)   **Pre-processing**
        The input data is then processed to enable the flow computations to proceed. Chiefly, this stage involves taking Fourier transforms of the terrain height and of the logarithm of the roughness length over the flow region. It also involves defining the depths h_m and ℓ of the **middle layer** and **inner region** over the terrain.

(iii)   **Calculation**
        Computation of the distribution of the *mean* flow, turbulence and mean streamlines on the internal calculation grid.

A3. Procedures and Algorithms for Computing Mean Flow over Hills

A3.1 Terrain height and lateral scale

(i)   Terrain is specified within a domain D which is a rectangle of side length $L_{*_x} \times L_{*_y}$ (typically $L_* \approx 10$ km).

(ii)   The height of the terrain $z_T(x)$ or $z_T(x, y)$ is specified on an irregularly-spaced mesh on a mesh scale of $\delta L_{*_x} \times \delta L_{*_y}$ (i.e. z_T is specified at points $[x_i, y_i]$). In general the input terrain may be an irregular mesh, but the calculation is carried out on a regular grid, with 16×16, 32×32, 64×64, 128×128 or 256×256 points.
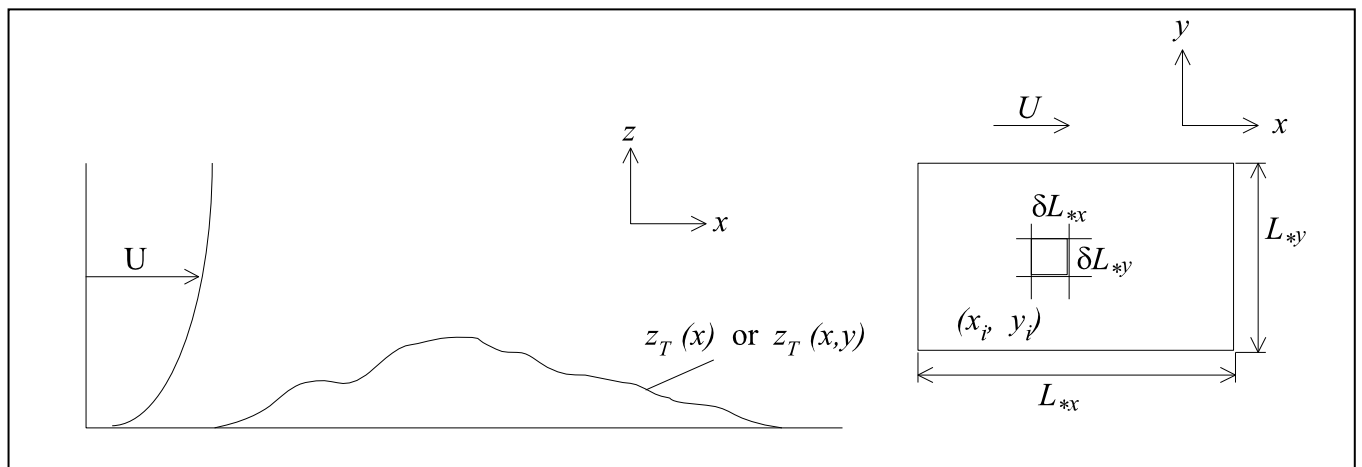

Figure A.1

A3.2 Roughness length z_0 over the terrain

The model can treat changes in surface roughness. Only the first-order solution is included in the current algorithm. Belcher et al [3] showed that when second-order effects are included the roughness changes lead to significant horizontal divergence which is absent from the first-order solution. Advice on the choice of z_0 for different fetches of actual terrain (country, sea, suburbs, etc) is given by, for example, Wieringa [9]. In the algorithms which follow z_0 is the surface roughness, which may vary with position, z_{0_u} is the value upstream and $\langle z_0 \rangle$ is the mean value over the calculation domain.

A3.3 Specifying the upwind meteorology

A3.3.1 Input profile of wind
The stability-dependent input wind profiles are defined in the specification for the boundary layer structure module (P09/01 'Boundary layer structure specification') and are the same as for flat terrain.

A3.3.2 Types of stratification

The type of stratification is defined in the outer layer. The middle and inner layers are effectively neutral in all conditions considered in this model. Note however, that the height of the middle and upper layer may be wave-number dependent. The buoyancy frequency is defined by

$$N^2 = -\frac{g}{\Theta}\frac{\partial\Theta}{\partial z} \tag{A3.1}$$

where Θ is the potential temperature.

Five stratification cases can be considered by FLOWSTAR, namely:

(i) S_0 - neutral

(ii) S_1 - uniform density, gradient and uniform wind speed (N/U constant with height);

(iii) S_2 - zero density gradient below inversion ($z < h_i$), density discontinuity ($z = h_i$) and uniform density gradient above inversion ($z > h_i$).

(iv) S_3 - strong inversion layer capping a uniformly stratified boundary layer, stable uniform density gradient below inversion;

(v) S_4 - lower layer gradually decreasing stratification up to an upper layer of constant stratification.

Only profiles (ii) and (iii) are currently used in ADMS.

A3.4   Calculating length scales and dimensionless groups

A3.4.1 Definition of the characteristic half length of the terrain L_1

$$L_1 = 1/\overline{k_1} \tag{A3.2}$$

where

$$\overline{k_1} = \frac{\int_{-\infty}^{\infty}\int_{-\infty}^{\infty} k_1\tilde{f}(k_1,k_2)dk_1,dk_2}{\int_{-\infty}^{\infty}\int_{-\infty}^{\infty}\tilde{f}(k_1,k_2)dk_1,dk_2} \tag{A3.3}$$

If the calculation mesh size selected is greater than 32×32, only the smallest 32 wavenumbers are included in this calculation. This ensures that L_1 represents the dominant features of the terrain.

The Fourier transform of the terrain is given by

$$\tilde{f} = \frac{1}{(2\pi)^2}\int_{-\infty}^{\infty}\int_{-\infty}^{\infty} f(x,y)e^{-i(k_1x+k_2y)}\,dxdy. \tag{A3.4}$$

A.3.4.2 Definition of the middle-layer height h_m

$$|S(h_m)|^2 = \frac{1}{L_1^2} \ where \ S^2 = (N/U)^2 - \frac{d^2U/dz^2}{U} \qquad\text{(A3.5)}$$

N and U have been defined as in Section A3.3.

Two values of h_m are taken for different ranges of wave number.

A typical wavenumber k_{12} is defined, where $k_{12} = \sqrt{k_1^2 + k_2^2}$.

For $k_{12} < 3/L_1$,

$$|S(h_m)|^2 = 1/L_1^2 \qquad\text{(A3.6)}$$

and for $k_{12} \geq 3/L_1$

$$S^2(h_m) = \big((3/L_1 + k_*)/2\big)^2 \qquad\text{(A3.7)}$$

where $k_* = 1/\delta L_*$.

A3.4.3 Definition of inner-layer thickness
The inner-layer thickness is defined for high and low wave numbers. For $k_{12} < 3/L_1$

$$\ell = 2\kappa^2 L_1/\ln(\ell/z_0) \qquad\text{(A3.8)}$$

and for $k_{12} \geq 3/L_1$

$$\ell = 2\kappa^2\big((3\bar{k}_{12} + k_*)/2\big)^{-1}/\ln(\ell/z_0) \qquad\text{(A3.9)}$$

A3.4.5 Roughness
The model uses the roughness data in the following manner for evaluation of the effect of surface roughness on the velocity.

(i)   A mean upstream roughness length z_{0u} is computed for the domain D. This is calculated by taking a weighted average of the mean roughness lengths on the two upstream edges of the domain.

(ii)   The surface roughness parameter is calculated as $m = \ln(z_0/z_{0u})$ for the grid points where z_0 is specified.

(iii)   The Fourier transform $\tilde{m}(k_1, k_2)$ is calculated.

A3.5 Calculating the velocity

For a summary of both the solution and the effects of stratification see section A2.

A3.5.1 Co-ordinates and velocity notation
We use displacement co-ordinates (x, y, Z) where Z, the height above the terrain, is defined as

$$Z = z - f(x, y) \qquad\text{(A3.10)}$$

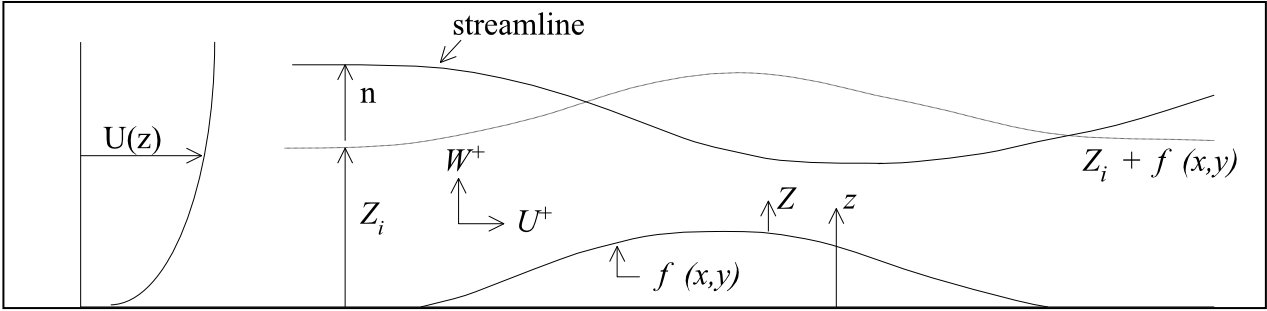Let $U_d(Z) = U(Z)$ be the upwind velocity at the height Z above the surface.

Figure A.2

The components of the velocities are

$$U^+(x, y, z) = U_d(Z) + u_d(x, y, Z) + u_R(x, y, Z) \tag{A3.11a}$$

$$W^+(x, y, z) = w_d(x, y, Z) + w_R(x, y, Z) \tag{A3.11b}$$

$$V^+(x, y, z) = v_d(x, y, Z) \tag{A3.11c}$$

where u_d, v_d and w_d are perturbations caused by the changes in elevation, and u_R and w_R are perturbations caused by roughness changes.

We denote the Fourier transform by ($\tilde{}$), thus

$$\tilde{U}^+(k_1, k_2, z) = \frac{1}{(2\pi)^2} \int_{-\infty}^{\infty} \int_{-\infty}^{\infty} U^+(x, y, z) e^{-i(k_1 x + k_2 y)} dx dy \tag{A3.12}$$

The general form of solutions for (u_d, v_d, w_d) (u_d, v_d, w_d) is:

$$\tilde{u}_d(k_1, k_2, Z) = \frac{\tilde{f}(k_1, k_2) k_1^2 |k_1|}{k_{12}^2} U_0 \begin{cases} \Gamma_{m,u} \text{ for } Z < h_m \\ \Gamma_{U,u} \text{ for } Z \geq h_m \end{cases} \tag{A3.13}$$

$$\tilde{v}_d(k_1, k_2, Z) = \frac{\tilde{f}(k_1, k_2) k_1 k_2 |k_1|}{k_{12}^2} U_0 \begin{cases} \Gamma_{m,v} \text{ for } Z < h_m \\ \Gamma_{U,u} \text{ for } Z \geq h_m \end{cases} \tag{A3.14}$$

$$\tilde{w}_d(k_1, k_2, Z) = \tilde{f}(k_1, k_2) i k_1 U_0 \Gamma_{U,w} \text{ for } Z \geq h_m \tag{A3.15}$$

where $U_0 = U(h_m)$. For $Z < h_m$, the expression for w_d is written in real space as

$$w_d = \left[(U + u_d) F^{-1}\left(i k_1 \tilde{f} \Gamma_{U,w}\right) + v_d F^{-1}\left(i k_2 \tilde{f} \Gamma_{U,w}\right) \right](1 - Z/h_m)$$

$$+\frac{UZ}{h_m}F^{-1}\left(ik_1\tilde{f}\Gamma_{U,w}\right) \tag{A3.16}$$

where F^{-1} represents the inverse Fourier transform and where $\Gamma_{U,u}$ etc. are factors defined in Section A3.5.3 below.

A3.5.2 General middle and inner-layer structure
Same form for most conditions when stratified (provided $Nh_m/U \leq 1$, and $N\ell/U \leq 1/2$).

Note:

$$k_{12} = \sqrt{k_1^2 + k_2^2}, \tag{A3.17}$$

$$\Gamma_{m,u} = \Gamma_{U,u}(Z)\Lambda J_u(Z)\left(1 - \frac{G_{u1}(Z) + G_{u2}(Z)}{J_u(Z)}\right) \tag{A3.18}$$

$$\Gamma_{m,v} = \Gamma_{U,u}(Z)\Lambda[1 - G_v(Z)] \tag{A3.19}$$

where G_{u2} is the approximate second-order correction term. The dimensionless parameters Λ, J_u, G_{u1}, G_{u2} and G_v are defined as follows.

For $\ell < Z < h_m$,

$$\Lambda = U_d(h_m)/U_d(Z)$$

$$J_u = 1 + \frac{k_{12}^2}{k_1^2}\frac{1}{\ln(Z/z_{0u})} \tag{A3.20}$$

$$G_{u1} = G_{u2} = G_v = 0$$

For $Z < l$,

$$\Lambda = U_d(h_m)/U_d(\ell)$$

$$J_u = 1 + \delta, \delta = 1/\ln(\ell/z_{0u})$$

$$G_{u1} = \delta(\ln(Z/\ell) - k')$$

$$G_{u2} = [2 + \delta(k' + 1)]K_0\left(\alpha_u\sqrt{i}\right)/K_0\left(\alpha_{u0}\sqrt{i}\right)$$

$$G_v(Z) = \delta\,4K_0\left(\alpha_v\sqrt{i}\right)U_d(Z)/U_d(\ell)$$

$$\alpha_u = 2\sqrt{k_1Z/\beta}, \quad \alpha_{u0} = 2\sqrt{k_1z_{ou}/\beta}, \quad \alpha_v = 2\sqrt{2k_1Z/\beta}$$

$$k' = k_{12}^2/k_1^2 - 1, \quad \beta = 2\kappa^2/\ln(\ell/z_{0u}), \quad \kappa = 0.4$$

and the modified Bessel function K_0 can be expressed as

$$K_0\left(\alpha\sqrt{i}\right) = \begin{cases} \mathrm{ker}(\alpha) + i\mathrm{kei}(\alpha), & \text{for } k_i > 0 \\ \mathrm{ker}(\alpha) - i\mathrm{kei}(\alpha), & \text{for } k_i < 0 \end{cases} \tag{A3.21}$$

where $\alpha = \alpha_u$ or $\alpha = \alpha_{u0}$ or $\alpha = \alpha_v$.

Note that the Kelvin functions, ker and kei, are computed using polynomial approximations [10].

To make sure the solutions are continuous at $Z = \ell$, we use blending functions to match the solutions in the inner region and middle layer. For $Z \leq \ell$

$$\Gamma_{m,u} = \Gamma_{m,u\ell}\left(1 - \frac{1}{2}\exp(-4(\ell - Z)/\ell)\right) + \frac{1}{2}\Gamma_{m,uh}\exp(-4(\ell - Z)/\ell)$$

$$\Gamma_{m,v} = \Gamma_{m,v\ell}\left(1 - \frac{1}{2}\exp(-4(\ell - Z)/\ell)\right) + \frac{1}{2}\Gamma_{m,vh}\exp(-4(\ell - Z)/\ell)$$

(A3.22)

and for $Z > l$

$$\Gamma_{m,u} = \Gamma_{m,uh}\left(1 - \frac{1}{2}\exp(-4(Z - \ell)/\ell)\right) + \frac{1}{2}\Gamma_{m,u\ell}\exp(-4(Z - \ell)/\ell)$$

$$\Gamma_{m,v} = \Gamma_{m,vh}\left(1 - \frac{1}{2}\exp(-4(Z - \ell)/\ell)\right) + \frac{1}{2}\Gamma_{m,v\ell}\exp(-4(Z - \ell)/\ell)$$

(A3.23)

where $\Gamma_{m,u\ell}$ and $\Gamma_{m,uh}$ are the functions in the inner region and middle layer respectively for the x-direction and $\Gamma_{m,v\ell}$ and $\Gamma_{m,vh}$ are the functions for the y-direction.

A3.5.3 Upper-layer functions for different stratification cases

(i)   **Neutral** (S_0)

$$\Gamma_{U,u} = \Gamma_{U,v} = \frac{k_{12}}{|k_1|}e^{-k_{12}Z}$$

(A3.24)

$$\Gamma_{U,w} = e^{-k_{12}Z}$$

(A3.25)

(ii)   **Stable** $(S_1$- Uniform $S(z)$ in upper layer)

$$S^2(z) = N^2/U^2(h_m)$$

(A3.26)

(note h_m is wavenumber dependent)

$$\Gamma_{U,u} = \Gamma_{U,v} = \frac{M_{12}}{|k_1|}e^{-M_{12}Z}$$

(A3.27)

$$\Gamma_{U,w} = e^{-M_{12}Z}$$

(A3.28)

If $|k_1| > S$

$$M_{12} = \sqrt{k_1^2 - S^2}(k_{12}/|k_1|)$$

(A3.29)

and $|k_1| < S$

$$M_{12} = \begin{cases} -i\sqrt{k_1^2 - S^2}(k_{12}/|k_1|) & \text{for } k_{12} > 0 \\ i\sqrt{k_1^2 - S^2}(k_{12}/|k_1|) & \text{for } k_{12} < 0 \end{cases}$$

<div align="right">(A3.30)</div>

(iii)   **Convective** (S_2 − Inversion at h_i with stable layer above and well-mixed layer below)

For $Z < h_m$,

$$S^2 = S_u^2 H(Z - h_i) + S_L^2 H(h_i - Z)$$

<div align="right">(A3.31)</div>

where $H(Z)$ is a step function, i.e.

$$H(Z) = \begin{cases} 1, & \text{for } Z > 0 \\ 0, & \text{for } Z < 0 \end{cases}$$

$S_u^2 = (N/U)_u^2$ - above inversion,

$S_L^2 = (N/U)_L^2$ - below inversion.

<div align="right">(A3.32)</div>

The Froude number of the inversion layer, F_i, is given by

$$F_i = \sqrt{\frac{U^2(h_i)\theta(h_i)}{h_i g \Delta\theta_i}}$$

<div align="right">(A3.33)</div>

In order to define F_i the user specifies the potential temperature step ($\Delta\theta_i$), $U(h_i)$ and the potential temperature $\theta(h_i)$.

For $h_m < Z < h_i$,

$$\Gamma_{U,u} = \Gamma_{U,v} = \frac{k_{12}}{|k_1|}(Ae^{-k_{12}Z} - Be^{k_{12}Z})$$

<div align="right">(A3.34a)</div>

$$\Gamma_{U,w} = Ae^{-k_{12}Z} - Be^{k_{12}Z}$$

<div align="right">(A3.34b)</div>

and for $Z > h_i$,

$$\Gamma_{U,u} = \Gamma_{U,v} = \frac{M_{12}H}{|k_1|}e^{-M_{12}(Z-h)}$$

<div align="right">(A3.35a)</div>

$$\Gamma_{U,w} = He^{-M_{12}(Z-h)}$$

<div align="right">(A3.35b)</div>

where

$$A = \frac{e^{k_{12}h_i}}{2\sinh(k_{12}h_i)}\left\{1 - [\coth(k_{12}h_i) - 1]\frac{k_{12}h_i}{D}\right\}$$

$$B = 1 - A$$

$$H = \frac{k_{12}h_i}{D}[\coth(k_{12}h_i) - 1]e^{k_{12}h_i}$$

<div align="right">(A3.36)</div>

$$D = M_{12}h_i + k_{12}h_i\coth(k_{12}h_i) - \frac{k_{12}^2}{k_1^2 F_i^2}$$

where D is a damping term introduced to avoid singularities due to trapped waves.

A3.6 Algorithm for roughness change

This is a first-order calculation, which gives the Fourier transform of the perturbation to U due to the roughness changes, u_R and w_R. ($v_R = 0$ to this order of accuracy). The Fourier transform of the roughness perturbation is largely determined by the roughness parameter m. The solutions are

$$\tilde{u}_R(k_1, k_2, Z) = -A\tilde{m}(k_1, k_2)K_0(2\sqrt{i\text{sign}(k_1)\zeta}) \tag{A3.37a}$$

$$\tilde{w}_R(k_1, k_2, Z) = -ik_1 A e^{-Z/l}\tilde{m}(k_1, k_2)\int_{z_0}^{Z} K_0\left(2\sqrt{i\text{sign}(k_1)\zeta}\right)dZ$$

$$= \frac{2\kappa^2 A e^{-Z/l}\tilde{m}(k_1, k_2)e^{-\zeta}}{\ln(\ell/z_{0u})}\frac{\partial K_0\left(2\sqrt{i\text{sign}(k_1)\zeta}\right)}{\partial\zeta}\Bigg|_{\zeta_0}^{\zeta} \tag{A3.37b}$$

where

$$\zeta = \frac{Z + z_{0u}}{l(k_1)} \ and \ \zeta_0 = \frac{z_{0bc}}{l(k_1)} \tag{A3.38a}$$

where z_{0u} is the upstream roughness (taken to be the mean value along the two upstream edges of the domain), and z_{0bc} is a 'boundary condition' roughness, set as follows:
- If z_{0u} is the minimum roughness over the domain, then z_{0bc} is the maximum roughness over the domain
- If z_{0u} is the maximum roughness over the domain, then z_{0bc} is the minimum roughness over the domain
- If z_{0u} is neither the maximum nor the minimum roughness, then z_{0bc} is the maximum roughness over the domain

and

$$A = \frac{u_*}{\kappa}\frac{1}{K_0\left(2\sqrt{i\text{sign}(k_1)\zeta_0}\right)} \tag{A3.38b}$$

$$l\left(\ln\left(\frac{l}{z_{0bc}}\right) - 1\right) + z_{0bc} = \frac{2\kappa^2\left(1 + \beta l^{\frac{2}{3}}\right)}{|k_1|} \tag{A3.38c}$$

$$\beta = 0.4\frac{2.1^2}{8\kappa h^{\frac{2}{3}}}\left(\frac{w_*^2}{u_*^2}\right) \tag{A3.38d}$$

so that $\ell(k_1)$ has to be evaluated for each wavenumber.

This means that the perturbation may be overestimated where the local roughness is less than the maximum roughness, but this can be counteracted (in a simple way) by constraining the vertical profile of U taking into account roughness changes only to lie between the two profiles

$$U(Z) = \frac{u_*}{\kappa}\ln\left(\frac{Z + z_{0u}}{z_{0max}}\right)f(stability) \tag{A3.38e}$$

and

$$U(Z) = \frac{u_*}{\kappa} \ln\left(\frac{Z + z_{0u}}{z_{0min}}\right) f(stability) \tag{A3.38f}$$

where z_{0max} and z_{0min} are the maximum and minimum roughness lengths over the domain, and the values of u_* used are those appropriate for each roughness, obtained by assuming that $U(H)$ is independent of the roughness (where H is boundary layer height), and assuming a neutral profile, which leads to the relationship

$$u_* = u_{*u} \frac{\ln\big((H + z_{0u})/z_{0u}\big)}{\ln\big((H + z_{0min})/z_{0min}\big)} \tag{A3.38g}$$

where u_{*u} is the upstream value of u_*.

A3.7 Algorithms for shear stress and surface shear stress

Near the surface, turbulence is approximately in local *equilibrium* so that shear stress can be modelled by the *mixing-length* closure, i.e. the perturbation shear stress can be written as

$$\tau_d = 2\kappa u_* Z \frac{\partial \Delta u}{\partial Z} e^{-Z/l} = 2\kappa u_* U_0 Z \frac{\partial u_d}{\partial Z} e^{-Z/l} \tag{A3.39}$$

where $\kappa = 0.4$ is the von Karman constant, u_* the upstream friction velocity, U_0 the upstream velocity at $Z = h_m$ and u_d the normalized perturbation of velocity, i.e. $u_d = \Delta u/U_0$.

The general forms of solution for (τ_{dx}, τ_{dy}):

$$\tilde{\tau}_{dx}(k_1, k_2, z) = \frac{\tilde{f}(k_1, k_2)k_1^2|k_1|}{k_{12}^2} 2\kappa u_* U_0 e^{-Z/l} \Gamma_{t,x}(k_1, Z) \tag{A3.40a}$$

$$\tilde{\tau}_{dy}(k_1, k_2, z) = \frac{\tilde{f}(k_1, k_2)k_1^2|k_1|}{k_{12}^2} \kappa u_* U_0 e^{-Z/l} \Gamma_{t,y}(k_1, Z) \tag{A3.40b}$$

Since the *mixing-length* closure is inadequate to model shear stress in the *upper layer*, in the following we give the algorithm of shear stress in the *middle and inner layer* only. For $\ell < Z \le h_m$:

$$\Gamma_{t,x} = -k_{12}Z \frac{k_{12}}{|k_1|} e^{-k_{12}Z} \Lambda_z J_u(Z) + \frac{k_{12}}{|k_1|} e^{-k_{12}Z} \Lambda_z J_{ut}(Z) \tag{A3.41}$$

$$\Gamma_{t,y} = -k_{12}Z \frac{k_{12}}{|k_1|} e^{-k_{12}Z} \Lambda_z J_v(Z) + \frac{k_{12}}{|k_1|} e^{-k_{12}Z} \Lambda_z J_{vt}(Z) \tag{A3.42}$$

where

$$\Lambda_z = U(h_m)/U(Z)$$

$$J_u = 1 + \frac{k_{12}^2}{k_1^2}\frac{1}{\ln(Z/z_{0u})}, \quad J_v = 1$$

$$J_{ut} = \frac{1}{\ln(Z/z_{0u})} - \frac{k_{12}^2}{k_1^2}\frac{2}{\ln^2(Z/z_{0u})}$$

$$J_{vt} = -\frac{1}{\ln(Z/z_{0u})}$$

(A3.43)

In the *inner region* $Z \leq \ell$:

$$\Gamma_{t,x} = -k_{12}Z\frac{k_{12}}{|k_1|}e^{-k_{12}Z}\Lambda_0 G_u(Z) + \frac{k_{12}}{|k_1|}e^{-k_{12}Z}\Lambda_0 G_{ut}(Z) \tag{A3.44a}$$

$$\Gamma_{t,y} = -k_{12}Z\frac{k_{12}}{|k_1|}e^{-k_{12}Z}\Lambda_0[1 - G_v(Z)] + \frac{k_{12}}{|k_1|}e^{-k_{12}Z}\Lambda_0 G_{vt}(Z) \tag{A3.44b}$$

where

$$\Lambda_0 = U(h_m)/U(\ell)$$

$$G_u = \frac{1}{\ln(\ell/z_{0u})} - \frac{\ln(Z/\ell) - k'}{\ln(\ell/z_{0u})} - \left\{2 + \frac{k' + 1}{\ln(\ell/z_0)}\right\}\frac{K_0(\alpha_u\sqrt{i})}{K_0(\alpha_{u0}\sqrt{i})}$$

$$G_{ut} = \frac{1}{\ln(\ell/z_{0u})} - \left\{2 + \frac{k' + 1}{\ln(\ell/z_{0u})}\right\}\frac{Z\partial K_0(\alpha_u\sqrt{i})/\partial Z}{K_0(\alpha_{u0}\sqrt{i})} \tag{A3.45}$$

$$G_v = 4\delta\, K_0(\alpha_v\sqrt{i})U(Z)/U(\ell)$$

$$G_{vt} = 4\delta\, Z(\partial K_0(\alpha_v\sqrt{i})/\partial Z)U(Z)/U(\ell) + 4\delta\, K_0(\alpha_v\sqrt{i})/\ln(\ell/z_o)$$

The surface shear stress is given by

$$\Gamma_{t,x,0} = 1 + \frac{1 + 4\gamma + 2\ln(ik_1)}{\ln(\ell/z_{0u})} \tag{A3.46a}$$

$$\Gamma_{t,y,0} = 1 \tag{A3.46b}$$

(for the definitions of some parameters see section A3.5.2.)

The algorithm for the shear stress perturbation due to roughness changes is given by

$$\tilde{\tau}_R(k_1, k_2, Z) = 2\kappa u_* Z e^{-Z/l}\frac{\partial \tilde{u}_R}{\partial Z}$$

$$= 2\kappa u_* A e^{-Z/l}\tilde{m}(k_1, k_2)\left(\sqrt{\zeta} - \frac{z_{0u}}{l\sqrt{\zeta}}\right)\sqrt{i\, sign(k_1)}\, K_1\left(2\sqrt{i\, sign(k_1)\zeta}\right)$$

$$\text{(A3.47)}$$

A3.8 Algorithms for turbulence

A3.8.1 Turbulent velocities

For the calculation of the turbulence components, estimates using the calculated shear stress are made in the inner region, while rapid distortion theory is used in the upper part of the middle and outer regions since the structure in these regions is determined by the distortion of the upwind turbulence structure. Between these two regions there is a layer where there are a number of effects determining the structure of the turbulence including advection, distortion, curvature and local non-linear effects [11]. It is not possible to calculate these effects within an approach suitable for diffusion, so since we know from observations that the turbulent velocities do not obtain locally large values in this region, we use a blending function to match the solution in the inner and outer regions across this layer [12].

Upwind the profiles are as defined in the Boundary Layer Structure Specification.

For the blending functions, we use in the inner region $(z < l)$

$$\alpha = 1 - \frac{1}{2}e^{-f_1((\ell - z)/\ell)} \qquad \text{(A3.48a)}$$

$$\beta = \frac{1}{2}e^{-f_1((\ell - z)/\ell)} \qquad \text{(A3.48b)}$$

and in the outer region $(z > l)$

$$\alpha = \frac{1}{2}e^{-f_1((z - \ell)/\ell)} \qquad \text{(A3.49a)}$$

$$\beta = 1 - \frac{1}{2}e^{-f_1((z - \ell)/\ell)} \qquad \text{(A3.49b)}$$

The expressions for the turbulence components over the hill are then

$$\sigma_u^2 = B_u^2\left[(u_*^2 + \alpha\tau_d + \tau_R) - \beta f_2 u_*^2\frac{u_d(Z)}{U_0(Z)}\right] + \sigma_{uc}^2\left[1 - f_2\frac{u_d(Z)}{U_0(Z)}\right] \qquad \text{(A3.50)}$$

$$\sigma_v^2 = B_v^2(u_*^2 + \alpha\tau_d + \tau_R) + \sigma_{uc}^2 \qquad \text{(A3.51)}$$

$$\sigma_w^2 = B_w^2\left[(u_*^2 + \alpha\tau_d + \tau_R) + \beta f_2 u_*^2\frac{u_d(Z)}{U_0(Z)} - f_3 H\left(\frac{-\partial f}{\partial x}\right)\cdot\frac{\partial f}{\partial x}e^{-z/h_m}\right]$$
$$+ \sigma_{wc}^2\left[1 + f_2\frac{u_d(Z)}{U_0(Z)}\right] \qquad \text{(A3.52)}$$

where for upwind isotropic turbulence $f_2 = 2/5$ and we have taken a value for the factor $f_1 = 2$.

The $\frac{\partial f}{\partial x}$ term in equation A3.52 has been introduced to account for the increase in vertical turbulence in the lee of the hill. The constant factor f_3 takes the value 5, and $H\left(\frac{-\partial f}{\partial x}\right)$ is the Heaviside step function of $\left(\frac{-\partial f}{\partial x}\right)$.

The suffixes N and C denote the upstream contribution from mechanically driven turbulence (u_* term) and convectively driven turbulence (w_* term).

The blending functions are such that the solutions are continuous at $Z = \ell$. The factors B_u, B_v, B_w have been introduced to allow for the decrease in the upwind turbulence energy with height ([3], 1988). They are defined as follows:

In convective or neutral conditions,

$$B_u = 2.5\left(1 - 0.8\frac{Z}{h}\right)$$

$$B_v = 2\left(1 - 0.8\frac{Z}{h}\right) \tag{A3.53a}$$

$$B_w = 1.3\left(1 - 0.8\frac{Z}{h}\right)$$

In stable conditions,

$$B_u = 2.5u_*\left(1 - 0.5\frac{Z}{h}\right)^{3/4}$$

$$B_v = 2u_*\left(1 - 0.5\frac{Z}{h}\right)^{3/4} \tag{A3.53b}$$

$$B_w = 1.3u_*\left(1 - 0.5\frac{Z}{h}\right)^{3/4}$$

In addition, a minimum value of 0.1 m/s is imposed on σ_u, σ_v, and σ_w.

In the above formulation for turbulence it is assumed that mechanically driven turbulence dominates convectively produced turbulence. However in moderate or strongly convective conditions this condition is no longer held. In those situations which occur in stratification case 2 when Monin-Obukhov length $L_{MO} < 0$, we include a contribution to the turbulent velocities due to convection; this contribution is not affected by the flow over the hills.

A3.8.2 Turbulent length scales
Following Weng et al [14], we assume a vertical length scale including the effects of local shear, i.e.

$$L_x^{(w)} = \left[\frac{A}{Z} + \frac{B\partial U/\partial Z}{\sigma_w} + \frac{4}{h}\right]^{-1} \tag{A3.54a}$$

where the constants are $A = 0.6$ and $B = 1.0$. For the transverse length scale an appropriate expression is

$$L_x^{(v)} = \frac{\sigma_{v0}^2}{\sigma_v^2} \; L_{x0}^{(v)} + \frac{\Delta\sigma_v^2}{\sigma_v^2} \; L_{x1}^{(v)} \tag{A3.54b}$$

where $L_{x1}^{(v)}$ is a local length scale which could be taken equal to $L_x^{(w)}$. However, for simplicity and in view of the fact that L_{x0} does not change significantly we take $L_x^{(v)} = L_x^{(w)}$. $L_{x0}^{(v)} = h/3$ ($h/L_{MO} < -0.3$), $L_{x0}^{(v)} = h/5$ ($h/L_{MO} \geq -0.3$), where h is the boundary layer depth.

APPENDIX B: Description of Stable Flow Algorithms

Contents

B1 Introduction

It is well established that when stable flows approach an isolated hill, the flow may divide with the air above a certain height, h_c, flowing over the hill and air below h_c flowing around the hill, see Figure B.1. h_c is the height of what is called the dividing streamline in 2-dimensions, or, in 3-dimensions, the dividing surface.
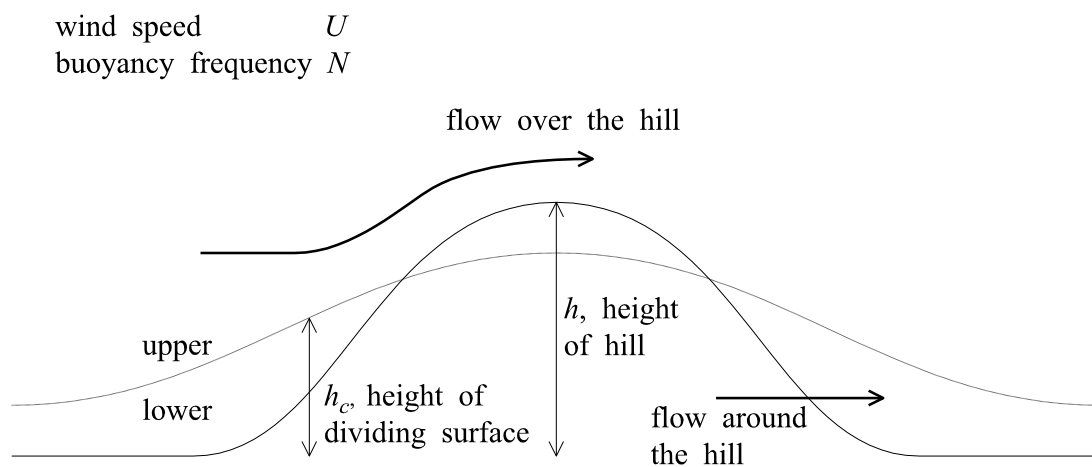

Figure B.1 Different flow regimes above and below the dividing surface

A critical value of 20 m is applied to the maximum dividing surface height, H_c. If $H_c > 20m$ then the method described in this section is applied based on a Gaussian shaped hill. (Note that variable roughness has no effect on the flow below the dividing streamline in this regime.) This stable flow field is used for the dispersion calculations over the whole domain. If $H_c < 20m$ then the usual FLOWSTAR flow field is used

In stable conditions, an adjusted buoyancy frequency, N_{adj}, is used in the FLOWSTAR solution, calculated by

$$N_{adj} = N(1 - 0.9\frac{H_c}{h_{max}})$$

where N is the standard buoyancy frequency and h_{max} is the height of the highest hill. This adjustment improves the FLOWSTAR solution for stable flows.

B2   Calculation of stable flow field

Suppose the input terrain data have height $f(x, y)$, z denotes height above sea level, Z the height above the terrain, the velocity field relative to the terrain at point (x, y, Z) is (u, v, W), and the velocity field relative to sea level is (u, v, w).

B2.1 Definition of idealised hill

The idealised hill is assumed to be Gaussian in shape with circular horizontal cross-section. The height of the hill is the maximum height of the input terrain, h_{max}, and is centred on the point where the input terrain maximum occurs, see Figure B.2. The height of the idealised hill, $h(x, y)$, where x and y are Cartesian co-ordinates with origin at the centre of the hill, is given by:

$$h(x, y) = h_{max}\exp\left(\frac{-(x^2 + y^2)}{L^2}\right)$$

where L is a characteristic length scale for the input terrain: $L = 0.5(L_1 + L_2)$, where L_1, the characteristic lengthscale in the alongwind direction, is given by A3.3, and L_2, the characteristic lengthscale in the crosswind direction, is calculated similarly using k_2 instead of k_1.
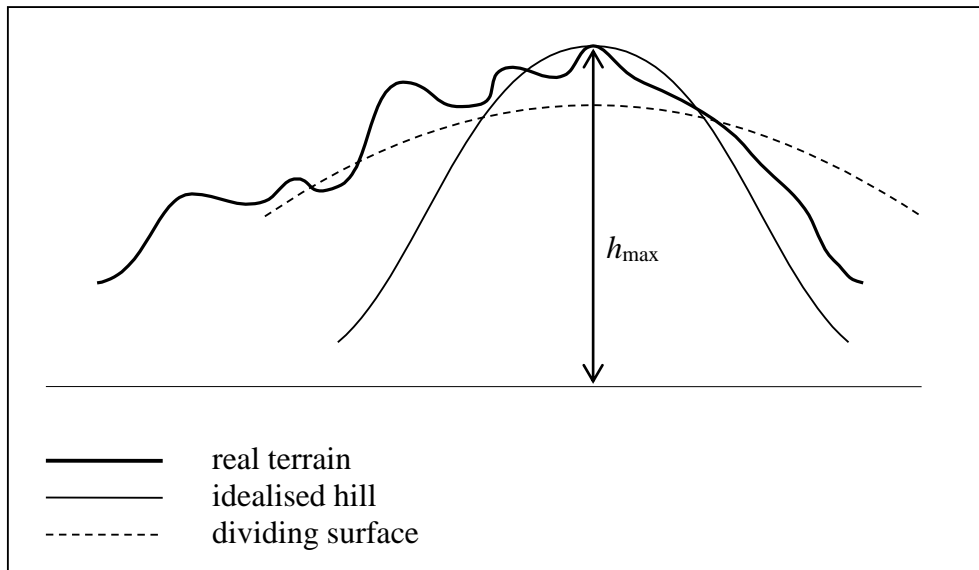
Figure B.2 Definition of idealised hill and dividing surface

B2.2 Definition of dividing surface

The dividing surface, illustrated in Figure B.2, is also assumed to be Gaussian in shape and its height $h_c(x, y)$ is given by:

$$h_c(x, y) = H_c \exp\left(\frac{-(x^2 + y^2)}{(\alpha L)^2}\right).$$

Here α is a constant set to 10, and H_c is the maximum height of the dividing surface which is defined by an energy balance equation which locates the lowest height at which the kinetic energy of an air parcel in the flow approaching the hill is equal to the potential energy attained by elevating an equivalent fluid parcel from this height to the top of the hill:

$$\frac{1}{2}U^2(H_c) = \int_{H_c}^{h_{max}} N^2(z)(h_{max} - z)dz$$

B2.3 Calculation of flow field

B2.3.1 Below the dividing surface
Below the dividing surface, the flow is two dimensional. The majority of the flow is potential flow. In a small region close to the terrain however (less than 10 m from the terrain surface) upstream flow is forced to flow parallel to the terrain. This means that the plume will travel around the hill. Figure B.3 gives a schematic diagram of this flow.
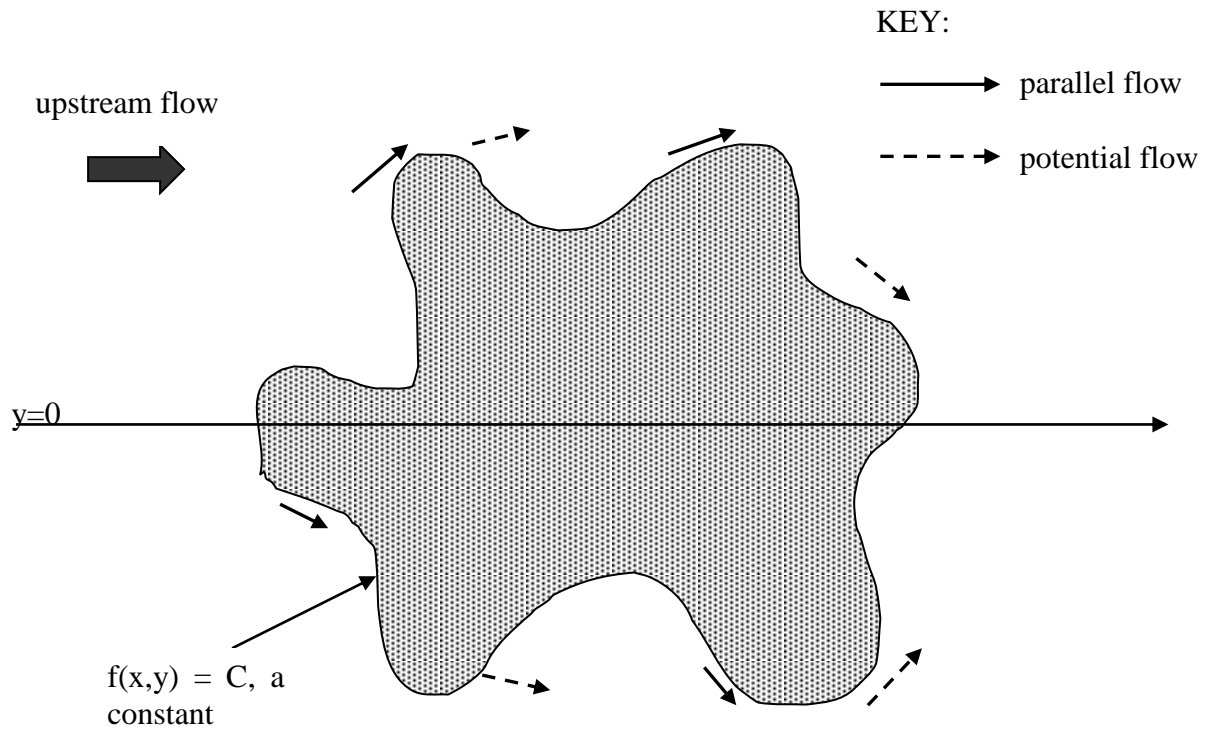
upstream flow

KEY:

→ parallel flow

⇢ potential flow

y=0

$f(x,y) = C$, a constant

Figure B.3 Stable flow close to the terrain

The mathematical formulation of the potential and parallel flows are given below.

Potential flow
We assume horizontal flow around a cone of radius r_0, where $r_0(z)$ is the radius of the idealised hill, at height z.

$$(u, v) = U_0(Z)\big(f_u(x, y), f_v(x, y)\big)$$

where

$$f_u(x, y) = 1 - \frac{r_0{}^2(x + y)(x - y)}{(x^2 + y^2)^2}$$

$$f_v(x, y) = \frac{-2xyr_0{}^2}{(x^2 + y^2)^2}$$

The vertical velocity is zero relative to the terrain, so

$$w = 0$$

Parallel flow
Upstream flow close to the terrain is parallel to the terrain. The flow field here takes the form

$$(u, v) = U_0(z)(\cos\theta, \sin\theta)$$

where

$$\tan\theta = \frac{-\partial f/\partial x}{\partial f/\partial y}$$

Again, the vertical velocity is zero relative to the terrain, so

$$w = 0$$

B2.3.2 Above the dividing surface
Above h_c the FLOWSTAR flow field is used, except in a thin layer close to the ground where a scaling is applied between flow parallel to the ground and the FLOWSTAR solution. The flow parallel to the ground is given by:

$$\boldsymbol{u = U_0(Z)}$$

$$\boldsymbol{v} = 0$$

$$\boldsymbol{w} = 0$$

B2.4 Calculation of turbulence parameters

The turbulence parameters are scaled by a factor S, which is the ratio of the terrain-influenced and unperturbed horizontal wind speeds, i.e.

$$u_* = Su_*{}^{flat}$$

$$\sigma_v = S\sigma_v{}^{flat}$$

$$\sigma_w = S\sigma_w{}^{flat}$$

where

$$S = \sqrt{\frac{u^2 + v^2}{U_0{}^2}} = \sqrt{f_u^2 + f_v^2}$$

APPENDIX C: Description of Reverse Flow algorithms

Contents

C1   Introduction

A source located wholly or partly within a region of recirculating flow may lead to high concentrations upstream of the source (relative to the free stream wind direction).

In ADMS it is assumed that the plume is well-mixed within the recirculation zone and is represented downwind of that region by dispersion from a virtual source or sources. This is closely analogous to the treatment of plumes entrained into the near wake of a building in the ADMS buildings module. However, unlike the buildings module, the case of a plume being partially entrained into the recirculation zone is not treated.

C2   General method

An 'effective source height' is defined, which includes the initial effects of buoyancy and momentum of the release. If the wind speed at the effective source is negative (i.e. the effective source is in a reverse flow region), then the full extent of the reverse flow region is found. An 'effective recirculation zone' is then defined (Figure C.1), throughout which the contaminant is assumed to be well-mixed. The concentration is assumed to be uniform within this 'effective recirculation zone'. The effective recirculation zone may be the same as the recirculation zone or may be contained within it, for instance if the zone is very wide.

At the downstream edge of this zone, the plume dispersion parameters (σ_y and σ_z) are estimated based on the cross-stream dimensions of the effective recirculation zone. These parameters are used in the subsequent calculations of plume concentration to represent dispersion from a 'virtual source' at the downstream edge of the zone, or, if the original source has significant crosswind extent, from a series of 'virtual sources'. The plume from each virtual source is assumed to be passive.

For an effective source outside the reverse flow region the plume dispersion calculations are influenced by a reverse flow region only if the plume centre line enters the region. No partial entrainment of the plume is considered. If reverse flow is encountered by the plume centreline, then the plume height is increased until it is

within a region of forward flow. The program will fail if this leads to a very large discontinuity in the plume height (i.e. if $\Delta z_p > \max(10 \text{ m}, 2z_p)$, where z_p is the height of the plume centreline).
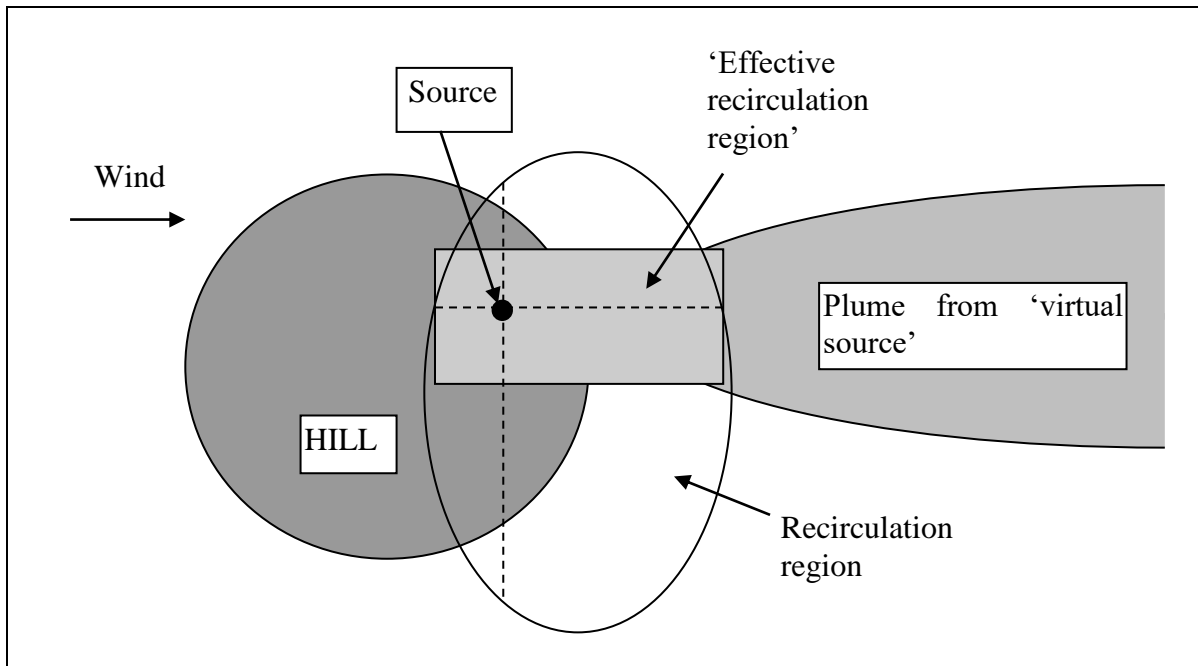

Figure C.1 The recirculating region and effective recirculating region

C3 Recirculating Region

The recirculating region is defined in the following manner:

(i)   The top and bottom of the region Z_{top} and Z_{base} are set to the first heights above and below the source height at which forward flow occurs.

(ii)   The length of the recirculation region (L_R) is calculated by finding the upwind and downwind edges of the region that lie along a wind-aligned trajectory that passes through the source, at a height $(Z_{top} + Z_{base})/2$.

(iii)   The width (W_R)of the region is calculated by finding the crosswind edges of the region that lie along a trajectory perpendicular to the mean flow passing through the source, at height $(Z_{top} + Z_{base})/2$.

By analogy with the building effects module, the recirculating flow region is assumed well-mixed out to a maximum width W_R' where

$$W_R' = \min\left(W_R, 3(Z_{top}\text{-}Z_{base}) + W_S\right).$$

where W_S is the crosswind width of the source. If $W_R \leq 3(Z_{top} + Z_{base})$, the effective well-mixed region, denoted R', is the same as the recirculation region, R. Otherwise, R' is located within R according to the lateral location of the source, y_s

such that R' is symmetric about the source position. If y_s is within half the effective width of a lateral edge of R, then R' extends W_R' from that edge.

The volume occupied by the effective recirculation region is then given by

$$V = W_R' \, L_R \left(Z_{top} - Z_{base}\right)$$

A residence time, T_R, is calculated for the emission inside the effective recirculating region:

$$T_R = \frac{\left(\left(Z_{\mathbf{top}} - Z_{\mathbf{base}}\right)W_R'\right)^{\frac{1}{2}}}{U\left(Z_{\mathbf{top}}\right)}$$

where $U\left(Z_{top}\right)$ is the mean upstream wind speed at height Z_{top}.

C4 Calculation of concentration

There are three cases to consider for the concentration calculations depending on the heights of the source and effective source relative to the reverse flow region.

(i)   ***The source and effective source are above the reverse flow region***
 Concentrations are calculated using the usual method for flow over complex terrain.

(ii)   ***The source is in the reverse flow region but the effective source is above it***
The initial plume height is set equal to the effective source height. Concentrations are calculated using the usual method for flow over complex terrain but with no further plume rise due to buoyancy or momentum effects.

(iii)   ***The source and effective source are within the reverse flow region***
The concentration calculation is split into two parts: the concentration in the reverse flow region and concentrations downstream of this region.

> [1] The mean concentration C_R inside the region R' is calculated by assuming that all the emissions are entrained and that the region is well-mixed. Then, applying a simple mass flux relationship
>
> $$C_R = \frac{QT_R}{V}$$
>
> where Q is the source mass emission rate, T_R is the residence time and V is the volume of the region.
>
> [2] Concentrations downstream of the recirculating region are determined by modelling a 'virtual' source at $\left(x_p, y_p, z_p\right)$ where
>
> $$x_p = x_{maxedge}$$

$$y_p = y_{maxedge} - W_R'/2 \qquad \text{if } y_{maxedge} - y_s < W_R'/2$$
$$y_p = y_{minedge} + W_R'/2 \qquad \text{if } y_s - y_{minedge} < W_R'/2$$
$$y_p = y_s \qquad\qquad \text{otherwise}$$

$$z_p = z_{slice}$$

where $x_{maxedge}$ is the downwind edge of the recirculating region, and $y_{maxedge}$ and $y_{minedge}$ are the cross-stream edges. (Co-ordinates (x, y) are wind-aligned.)

It is assumed that the plume parameters take the following values at the virtual source location:

$$\sigma_y = \frac{1}{\sqrt{3}} \frac{W_R'}{2} = \sigma_v t_{y0}$$

$$\sigma_z = \frac{1}{\sqrt{3}} Z_{max} = \sigma_w t_{z0}$$

where t_{y0}, t_{z0} are 'virtual' times used in the calculation of σ_y and σ_z, respectively at a height z_{slice}.

z_{slice} is the halfway height of the reverse flow region, i.e.

$$z_{slice} = \frac{z_{top} + z_{base}}{2}$$

Flat terrain values of σ_v and σ_w at height z_{slice} are used to calculate t_{y0} and t_{z0}.

The plume from the virtual source is assumed not to experience any plume rise because of the large dilution in the reverse flow region, nullifying the effect of the buoyancy force.

For line, area or volume sources, it is possible that the source is partly within a region of reverse flow, or spans more than one reverse flow region. In these circumstances the parts of the source that are within regions of reverse flow and those that are not are treated separately.